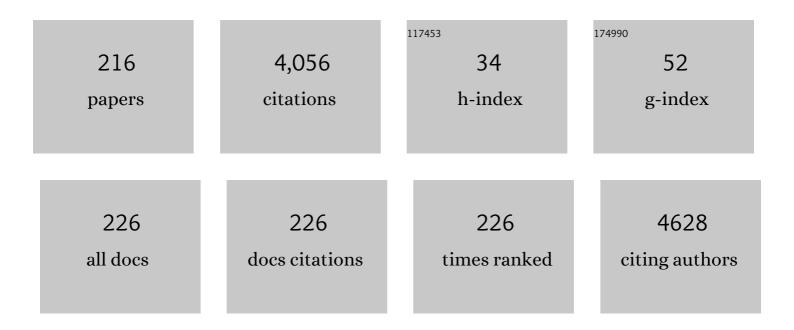
List of Publications by Year in descending order

Source: https://exaly.com/author-pdf/142405/publications.pdf Version: 2024-02-01



#	Article	IF	CITATIONS
1	A Novel Pt–TiO ₂ Heterostructure with Oxygenâ€Deficient Layer as Bilaterally Enhanced Sonosensitizer for Synergistic Chemoâ€6onodynamic Cancer Therapy. Advanced Functional Materials, 2020, 30, 1908598.	7.8	226
2	Recent developments in electrode materials for potassium-ion batteries. Journal of Materials Chemistry A, 2019, 7, 4334-4352.	5.2	214
3	The correlation between acoustic cavitation and sonoporation involved in ultrasound-mediated DNA transfection with polyethylenimine (PEI) in vitro. Journal of Controlled Release, 2010, 145, 40-48.	4.8	162
4	Experimental study on cell self-sealing during sonoporation. Journal of Controlled Release, 2008, 131, 205-210.	4.8	98
5	Mechanisms underlying sonoporation: Interaction between microbubbles and cells. Ultrasonics Sonochemistry, 2020, 67, 105096.	3.8	90
6	Asymmetric Synthesis of Tetrahydroindolizines by Bimetallic Relay Catalyzed Cycloaddition of Pyridinium Ylides. Angewandte Chemie - International Edition, 2018, 57, 12323-12327.	7.2	87
7	Microbubble-induced sonoporation involved in ultrasound-mediated DNA transfection in vitro at low acoustic pressures. Journal of Biomechanics, 2012, 45, 1339-1345.	0.9	86
8	Sonoporation-induced cell membrane permeabilization and cytoskeleton disassembly at varied acoustic and microbubble-cell parameters. Scientific Reports, 2018, 8, 3885.	1.6	81
9	High thermoelectric performance of superionic argyrodite compound Ag ₈ SnSe ₆ . Journal of Materials Chemistry C, 2016, 4, 5806-5813.	2.7	77
10	Low-frequency anechoic metasurface based on coiled channel of gradient cross-section. Applied Physics Letters, 2019, 114, .	1.5	71
11	Transcriptome comparison reveals a genetic network regulating the lower temperature limit in fish. Scientific Reports, 2016, 6, 28952.	1.6	66
12	Experimental investigation of the acoustic nonlinearity parameter tomography for excised pathological biological tissues. Ultrasound in Medicine and Biology, 1999, 25, 593-599.	0.7	62
13	"Two-in-One―Fabrication of Fe ₃ O ₄ /MePEG-PLA Composite Nanocapsules as a Potential Ultrasonic/MRI Dual Contrast Agent. Langmuir, 2011, 27, 12134-12142.	1.6	60
14	Acoustic non-diffracting Airy beam. Journal of Applied Physics, 2015, 117, .	1.1	58
15	Diversified Transformations of Tetrahydroindolizines to Construct Chiral 3-Arylindolizines and Dicarbofunctionalized 1,5-Diketones. Journal of the American Chemical Society, 2020, 142, 15975-15985.	6.6	58
16	Reduced graphene oxide modified mesoporous FeNi alloy/carbon microspheres for enhanced broadband electromagnetic wave absorbers. Materials Chemistry Frontiers, 2017, 1, 1786-1794.	3.2	56
17	Asymmetric [3 + 2] Cycloaddition of Methyleneindolinones with <i>N</i> , <i>N</i> ′-Cyclic Azomethine Imines Catalyzed by a <i>N</i> , <i>N</i> ′-Dioxide–Mg(OTf) ₂ Complex. Journal of Organic Chemistry, 2015, 80, 9691-9699.	1.7	53
18	Synthesis of H ₂ V ₃ O ₈ /Reduced Graphene Oxide Composite as a Promising Cathode Material for Lithiumâ€ion Batteries. ChemPlusChem, 2014, 79, 447-453.	1.3	52

#	Article	IF	CITATIONS
19	Study of acoustic nonlinearity parameter imaging methods in reflection mode for biological tissues. Journal of the Acoustical Society of America, 2004, 116, 1819-1825.	0.5	49
20	Double-scattering/reflection in a Single Nanoparticle for Intensified Ultrasound Imaging. Scientific Reports, 2015, 5, 8766.	1.6	49
21	Investigation on the inertial cavitation threshold and shell properties of commercialized ultrasound contrast agent microbubbles. Journal of the Acoustical Society of America, 2013, 134, 1622-1631.	0.5	47
22	Improvement of tissue harmonic imaging using the pulse-inversion technique. Ultrasound in Medicine and Biology, 2005, 31, 889-894.	0.7	46
23	Phase-coded approach for controllable generation of acoustical vortices. Journal of Applied Physics, 2013, 113, .	1.1	43
24	A large areal capacitance structural supercapacitor with a 3D rGO@MnO ₂ foam electrode and polyacrylic acid–Portland cement–KOH electrolyte. Journal of Materials Chemistry A, 2020, 8, 12586-12593.	5.2	43
25	Acoustic nonlinearity parameter tomography for biological specimens via measurements of the second harmonics. Journal of the Acoustical Society of America, 1996, 99, 2397-2402.	0.5	41
26	Cell-cycle-specific Cellular Responses to Sonoporation. Theranostics, 2017, 7, 4894-4908.	4.6	41
27	Modelling of SAW-PDMS acoustofluidics: physical fields and particle motions influenced by different descriptions of the PDMS domain. Lab on A Chip, 2019, 19, 2728-2740.	3.1	39
28	Global identification of the genetic networks and <i>cis</i> -regulatory elements of the cold response in zebrafish. Nucleic Acids Research, 2015, 43, 9198-9213.	6.5	38
29	Enantioselective [2+2] Photocycloaddition Reactions of Enones and Olefins with Visible Light Mediated by <i>N</i> N′â€Dioxide–Metal Complexes. Chemistry - A European Journal, 2018, 24, 19361-19367.	1.7	38
30	Photo- and Sono-Dynamic Therapy: A Review of Mechanisms and Considerations for Pharmacological Agents Used in Therapy Incorporating Light and Sound. Current Pharmaceutical Design, 2019, 25, 401-412.	0.9	38
31	Enhancement of subharmonic emission from encapsulated microbubbles by using a chirp excitation technique. Physics in Medicine and Biology, 2007, 52, 5531-5544.	1.6	37
32	Chiral N,N′-dioxide/Co(<scp>ii</scp>)-promoted asymmetric 1,3-dipolar cycloaddition of nitrones with methyleneindolinones. Chemical Communications, 2017, 53, 7925-7928.	2.2	37
33	Interaction between cavitation microbubble and cell: A simulation of sonoporation using boundary element method (BEM). Ultrasonics Sonochemistry, 2017, 39, 863-871.	3.8	37
34	Enantioselective Synthesis of 2,2,3-Trisubstituted Indolines via Bimetallic Relay Catalysis of α-Diazoketones with Enones. Organic Letters, 2018, 20, 4536-4539.	2.4	37
35	Fine Physical and Genetic Mapping of Powdery Mildew Resistance Gene MlIW172 Originating from Wild Emmer (Triticum dicoccoides). PLoS ONE, 2014, 9, e100160.	1.1	36
36	Harmonic responses and cavitation activity of encapsulated microbubbles coupled with magnetic nanoparticles. Ultrasonics Sonochemistry, 2016, 29, 309-316.	3.8	36

#	Article	IF	CITATIONS
37	Electro-acupuncture attenuates the mice premature ovarian failure via mediating PI3K/AKT/mTOR pathway. Life Sciences, 2019, 217, 169-175.	2.0	35
38	Composite phase change material based on reduced graphene oxide/expanded graphite aerogel with improved thermal properties and shapeâ€stability. International Journal of Energy Research, 2020, 44, 242-256.	2.2	35
39	Microbubble oscillating in a microvessel filled with viscous fluid: A finite element modeling study. Ultrasonics, 2016, 66, 54-64.	2.1	31
40	Ultrasound-Enhanced Protective Effect of Tetramethylpyrazine against Cerebral Ischemia/Reperfusion Injury. PLoS ONE, 2014, 9, e113673.	1,1	31
41	Investigation into the Effect of Acoustic Radiation Force and Acoustic Streaming on Particle Patterning in Acoustic Standing Wave Fields. Sensors, 2017, 17, 1664.	2.1	28
42	Mechanical and dynamic characteristics of encapsulated microbubbles coupled by magnetic nanoparticles as multifunctional imaging and drug delivery agents. Physics in Medicine and Biology, 2014, 59, 6729-6747.	1.6	26
43	Experimental imaging of the acoustic nonlinearity parameter B/A for biological tissues via a parametric array. Ultrasound in Medicine and Biology, 2001, 27, 1359-1365.	0.7	25
44	Noninvasive Estimation of Temperature Elevations in Biological Tissues Using Acoustic Nonlinearity Parameter Imaging. Ultrasound in Medicine and Biology, 2008, 34, 414-424.	0.7	25
45	Detection of fatigue-induced micro-cracks in a pipe by using time-reversed nonlinear guided waves: A three-dimensional model study. Ultrasonics, 2012, 52, 912-919.	2.1	25
46	Modeling complicated rheological behaviors in encapsulating shells of lipid-coated microbubbles accounting for nonlinear changes of both shell viscosity and elasticity. Physics in Medicine and Biology, 2013, 58, 985-998.	1.6	25
47	Asymmetric Synthesis of Tetrahydroindolizines by Bimetallic Relay Catalyzed Cycloaddition of Pyridinium Ylides. Angewandte Chemie, 2018, 130, 12503-12507.	1.6	25
48	Fourier and non-Fourier bio-heat transfer models to predict <i>ex vivo</i> temperature response to focused ultrasound heating. Journal of Applied Physics, 2018, 123, .	1.1	24
49	Principle and performance of orbital angular momentum communication of acoustic vortex beams based on single-ring transceiver arrays. Journal of Applied Physics, 2020, 127, .	1.1	23
50	The experimental investigation of ultrasonic properties for a sonicated contrast agent and its application in biomedicine. Ultrasound in Medicine and Biology, 2000, 26, 347-351.	0.7	22
51	Controllable in vivo hyperthermia effect induced by pulsed high intensity focused ultrasound with low duty cycles. Applied Physics Letters, 2012, 101, 124102.	1.5	22
52	Acoustic dipole radiation based electrical impedance contrast imaging approach of magnetoacoustic tomography with magnetic induction. Medical Physics, 2013, 40, 052902.	1.6	22
53	Acoustic dipole radiation based conductivity image reconstruction for magnetoacoustic tomography with magnetic induction. Applied Physics Letters, 2012, 100, 024105.	1.5	21
54	Ultrasound-assisted permeability improvement and acoustic characterization for solid-state fabricated PLA foams. Ultrasonics Sonochemistry, 2013, 20, 137-143.	3.8	21

#	Article	IF	CITATIONS
55	Enhanced porosity and permeability of three-dimensional alginate scaffolds via acoustic microstreaming induced by low-intensity pulsed ultrasound. Ultrasonics Sonochemistry, 2017, 37, 279-285.	3.8	21
56	Deep-level stereoscopic multiple traps of acoustic vortices. Journal of Applied Physics, 2017, 121, 164901.	1.1	20
57	Ambient pressure dependence of the ultra-harmonic response from contrast microbubbles. Journal of the Acoustical Society of America, 2012, 131, 4358-4364.	0.5	18
58	Construction of multifunctional films based on graphene–TiO2 composite materials for strain sensing and photodegradation. RSC Advances, 2015, 5, 104785-104791.	1.7	18
59	Simultaneous synthesis of diverse graphene via electrochemical reduction of graphene oxide. Journal of Applied Electrochemistry, 2015, 45, 453-462.	1.5	18
60	Prediction of suspicious thyroid nodule using artificial neural network based on radiofrequency ultrasound and conventional ultrasound: A preliminary study. Ultrasonics, 2019, 99, 105951.	2.1	18
61	Robust Ruddlesdenâ€Popper phase Sr ₃ Fe _{1.3} Mo _{0.5} N _{i0.2} O _{7â€î} decorated with inâ€situ exsolved Ni nanoparticles as an efficient anode for hydrocarbon fueled solid oxide fuel cells. SusMat. 2022. 2. 487-501.	7.8	18
62	Preparation and Thermal Properties of Graphene Oxide–Microencapsulated Phase Change Materials. Nanoscale and Microscale Thermophysical Engineering, 2016, 20, 147-157.	1.4	17
63	Preventing microbial biofilms on catheter tubes using ultrasonic guided waves. Scientific Reports, 2017, 7, 616.	1.6	17
64	Acoustic Characterization and Enhanced Ultrasound Imaging of Long irculating Lipidâ€Coated Microbubbles. Journal of Ultrasound in Medicine, 2018, 37, 1243-1256.	0.8	17
65	Acoustic source analysis of magnetoacoustic tomography with magnetic induction for conductivity gradual-varying tissues. IEEE Transactions on Biomedical Engineering, 2015, 63, 1-1.	2.5	16
66	Acoustic radiation torque of an acoustic-vortex spanner exerted on axisymmetric objects. Applied Physics Letters, 2018, 112, 254101.	1.5	16
67	<i>N</i> , <i>N</i> â€2-Dioxide/Gd(OTf) ₃ Complex-Promoted Asymmetric Aldol Reaction of Silyl Ketene Imines with Isatins: Water Plays an Important Role. Organic Letters, 2018, 20, 5314-5318.	2.4	16
68	Noninvasive Treatment-Efficacy Evaluation for HIFU Therapy Based on Magneto-Acousto-Electrical Tomography. IEEE Transactions on Biomedical Engineering, 2019, 66, 666-674.	2.5	16
69	Acoustic Characterization of Polydimethylsiloxane for Microscale Acoustofluidics. Physical Review Applied, 2020, 13, .	1.5	16
70	A dual-frequency excitation technique for enhancing the sub-harmonic emission from encapsulated microbubbles. Physics in Medicine and Biology, 2009, 54, 4257-4272.	1.6	15
71	Comparative Study of Lesions Created by High-Intensity Focused Ultrasound Using Sequential Discrete and Continuous Scanning Strategies. IEEE Transactions on Biomedical Engineering, 2013, 60, 763-769.	2.5	15
72	Pressure distribution based optimization of phase-coded acoustical vortices. Journal of Applied Physics, 2014, 115, .	1.1	15

#	Article	IF	CITATIONS
73	Self-assembly of new M(ii) coordination polymers based on asymmetric 1,3,4-oxadiazole-containing ligands: effect of counterions and magnetic properties. CrystEngComm, 2017, 19, 5864-5872.	1.3	15
74	Enantioselective [3 + 2] cycloaddition and rearrangement of thiazolium salts to synthesize thiazole and 1,4-thiazine derivatives. Organic Chemistry Frontiers, 2018, 5, 2126-2131.	2.3	15
75	Low‑intensity pulsed ultrasound promotes apoptosis and inhibits angiogenesis via p38 signaling‑mediated endoplasmic reticulum stress in human endothelial cells. Molecular Medicine Reports, 2019, 19, 4645-4654.	1.1	15
76	Effects of active noise cancelling headphones on speech recognition. Applied Acoustics, 2020, 165, 107335.	1.7	15
77	Near-field multiple traps of paraxial acoustic vortices with strengthened gradient force generated by sector transducer array. Journal of Applied Physics, 2018, 123, .	1.1	14
78	A facile template free synthesis of porous carbon nanospheres with high capacitive performance. Science China Chemistry, 2018, 61, 538-544.	4.2	14
79	The influence of droplet concentration on phase change and inertial cavitation thresholds associated with acoustic droplet vaporization. Journal of the Acoustical Society of America, 2020, 148, EL375-EL381.	0.5	14
80	An intelligent platform for ultrasound diagnosis of thyroid nodules. Scientific Reports, 2020, 10, 13223.	1.6	14
81	Asymmetric Catalytic Epoxidation of Terminal Enones for the Synthesis of Triazole Antifungal Agents. Organic Letters, 2021, 23, 6961-6966.	2.4	14
82	Lowâ€intensity pulsed ultrasound prevents prolonged hypoxiaâ€induced cardiac fibrosis through HIFâ€Iα/DNMT3a pathway via a TRAAKâ€dependent manner. Clinical and Experimental Pharmacology and Physiology, 2021, 48, 1500-1514.	0.9	14
83	Cavitation-facilitated transmembrane permeability enhancement induced by acoustically vaporized nanodroplets. Ultrasonics Sonochemistry, 2021, 79, 105790.	3.8	14
84	Microstreaming velocity field and shear stress created by an oscillating encapsulated microbubble near a cell membrane. Chinese Physics B, 2014, 23, 124302.	0.7	13
85	Linear phase distribution of acoustical vortices. Journal of Applied Physics, 2014, 116, 024905.	1.1	13
86	Ultrasound-Enhanced Protective Effect of Tetramethylpyrazine via the ROS/HIF-1A Signaling Pathway in an in Vitro Cerebral Ischemia/Reperfusion Injury Model. Ultrasound in Medicine and Biology, 2018, 44, 1786-1798.	0.7	13
87	The enhanced HIFU-induced thermal effect via magnetic ultrasound contrast agent microbubbles. Ultrasonics Sonochemistry, 2018, 49, 111-117.	3.8	13
88	Cell-cycle-dependences of membrane permeability and viability observed for HeLa cells undergoing multi-bubble-cell interactions. Ultrasonics Sonochemistry, 2019, 53, 178-186.	3.8	13
89	Low-intensity pulsed ultrasound ameliorates angiotensin II-induced cardiac fibrosis by alleviating inflammation via a caveolin-1-dependent pathway. Journal of Zhejiang University: Science B, 2021, 22, 818-838.	1.3	13
90	Low-intensity pulsed ultrasound suppresses proliferation and promotes apoptosis via p38 MAPK signaling in rat visceral preadipocytes. American Journal of Translational Research (discontinued), 2018, 10, 948-956.	0.0	13

#	Article	IF	CITATIONS
91	Acoustic characterization of high intensity focused ultrasound fields generated from a transmitter with a large aperture. Journal of Applied Physics, 2014, 115, 114902.	1.1	12
92	Reception pattern influence on magnetoacoustic tomography with magnetic induction. Chinese Physics B, 2015, 24, 014302.	0.7	12
93	An Online Impedance Analysis and Matching System for Ultrasonic Transducers. IEEE Transactions on Ultrasonics, Ferroelectrics, and Frequency Control, 2019, 66, 591-599.	1.7	12
94	Focused acoustic vortex generated by a circular array of planar sector transducers using an acoustic lens, and its application in object manipulation. Journal of Applied Physics, 2020, 128, .	1.1	12
95	Polymeric microcapsules with internal cavities for ultrasonic imaging: efficient fabrication and physical characterization. Colloid and Polymer Science, 2009, 287, 683-693.	1.0	11
96	Low intensity pulse ultrasound stimulate chondrocytes growth in a 3-D alginate scaffold through improved porosity and permeability. Ultrasonics, 2015, 58, 43-52.	2.1	11
97	Characterization of mechanical properties of hybrid contrast agents by combining atomic force microscopy with acoustic/optic assessments. Journal of Biomechanics, 2016, 49, 319-325.	0.9	11
98	Two-Dimensional Mapping Separating the Acoustic Radiation Force and Streaming in Microfluidics. Physical Review Applied, 2019, 11, .	1.5	11
99	Theoretical and experimental study of the third-order nonlinearity parameter C/A for biological media. Physica D: Nonlinear Phenomena, 2007, 228, 172-178.	1.3	10
100	Exploring the structure–property relationships of ultrasonic/MRI dual imaging magnetite/PLA microbubbles: magnetite@Cavity versus magnetite@Shell systems. Colloid and Polymer Science, 2012, 290, 1617-1626.	1.0	10
101	Kinetic evaluation of the size-dependent decomposition performance of solvent-free microcellular polylactic acid foams. Science Bulletin, 2012, 57, 83-89.	1.7	10
102	Transducer selection and application in magnetoacoustic tomography with magnetic induction. Journal of Applied Physics, 2016, 119, 094903.	1.1	10
103	Quantitative assessment of acoustic pressure in one-dimensional acoustofluidic devices driven by standing surface acoustic waves. Applied Physics Letters, 2017, 111, .	1.5	10
104	Prediction of HIFU Propagation in a Dispersive Medium via Khokhlov–Zabolotskaya–Kuznetsov Model Combined with a Fractional Order Derivative. Applied Sciences (Switzerland), 2018, 8, 609.	1.3	10
105	Auto-focusing acoustic-vortex tweezers for obstacle-circumventing manipulation. Journal of Applied Physics, 2021, 130, .	1.1	10
106	Acoustic focusing of sub-wavelength scale achieved by multiple Fabry-Perot resonance effect. Journal of Applied Physics, 2014, 115, .	1.1	9
107	Variations in Temperature Distribution and Tissue Lesion Formation Induced by Tissue Inhomogeneity for Therapeutic Ultrasound. Ultrasound in Medicine and Biology, 2014, 40, 1857-1868.	0.7	9
108	Second harmonic magnetoacoustic responses of magnetic nanoparticles in magnetoacoustic tomography with magnetic induction*. Chinese Physics B, 2020, 29, 034302.	0.7	9

#	Article	IF	CITATIONS
109	Spectrum Decomposition-Based Orbital Angular Momentum Communication of Acoustic Vortex Beams Using Single-Ring Transceiver Arrays. IEEE Transactions on Ultrasonics, Ferroelectrics, and Frequency Control, 2021, 68, 1399-1407.	1.7	9
110	Phase Change Materials Composite Based on Hybrid Aerogel with Anisotropic Microstructure. Materials, 2021, 14, 777.	1.3	9
111	Subharmonic and ultraharmonic emissions based on the nonlinear oscillation of encapsulated microbubbles in ultrasound contrast agents. Science Bulletin, 2005, 50, 1975-1978.	4.3	8
112	Performance evaluation of eigendecomposition-based adaptive clutter filter for color flow imaging. Ultrasonics, 2006, 44, e67-e71.	2.1	8
113	Quantitative evaluation of fracture healing process of long bones using guided ultrasound waves: A computational feasibility study. Journal of the Acoustical Society of America, 2009, 125, 2834-2837.	0.5	8
114	Sub-wavelength ultrasonic therapy using a spherical cavity transducer with open ends. Applied Physics Letters, 2013, 102, .	1.5	8
115	Influence of temperature and voltage on electrochemical reduction of graphene oxide. Bulletin of Materials Science, 2014, 37, 629-634.	0.8	8
116	Uniform tissue lesion formation induced by high-intensity focused ultrasound along a spiral pathway. Ultrasonics, 2017, 77, 38-46.	2.1	8
117	Noninvasive treatment efficacy monitoring and dose control for high-intensity focused ultrasound therapy using relative electrical impedance variation. Chinese Physics B, 2017, 26, 054302.	0.7	8
118	Investigation of a multi-element focused air-coupled transducer. AIP Advances, 2018, 8, .	0.6	8
119	Enhanced eradication of Pseudomonas aeruginosa bio-films by using ultrasound combined with neutrophil and antibiotics. Applied Acoustics, 2019, 152, 101-109.	1.7	8
120	Chirp excitation technique to enhance microbubble displacement induced by ultrasound radiation force. Journal of the Acoustical Society of America, 2009, 125, 1410-1415.	0.5	7
121	Effect of microbubble-enhanced ultrasound on percutaneous ethanol ablation of rat walker-256 tumour. European Radiology, 2016, 26, 3017-3025.	2.3	7
122	Acoustic field of an ultrasonic cavity resonator with two open ends: Experimental measurements and lattice Boltzmann method modeling. Journal of Applied Physics, 2017, 121, .	1.1	7
123	Interaction between encapsulated microbubbles: A finite element modelling study. Chinese Physics B, 2018, 27, 084302.	0.7	7
124	Pr and Mo Coâ€Doped SrFeO _{3–<i>δ</i>} as an Efficient Cathode for Pure CO ₂ Reduction Reaction in a Solid Oxide Electrolysis Cell. Energy Technology, 2020, 8, 2000539.	1.8	7
125	A FVCOM study of the potential coastal flooding in apponagansett bay and clarks cove, Dartmouth Town (MA). Natural Hazards, 2020, 103, 2787-2809.	1.6	7
126	Study on the variation of rock pore structure after polymer gel flooding. E-Polymers, 2020, 20, 32-38.	1.3	7

#	Article	IF	CITATIONS
127	Contact Nonlinear Acoustic Diode. Scientific Reports, 2020, 10, 2564.	1.6	7
128	Latency prediction of earmuff using a lumped parameter model. Applied Acoustics, 2021, 176, 107870.	1.7	7
129	The influence of ultrasound-induced microbubble cavitation on the viability, migration and cell cycle distribution of melanoma cells. Applied Acoustics, 2021, 179, 108056.	1.7	7
130	Automatic identification of triple negative breast cancer in ultrasonography using a deep convolutional neural network. Scientific Reports, 2021, 11, 20474.	1.6	7
131	Relationship between the temperature and the acoustic nonlinearity parameter in biological tissues. Science Bulletin, 2004, 49, 2360-2363.	1.7	6
132	Ti-Si-N films prepared by magnetron sputtering. Rare Metals, 2012, 31, 183-188.	3.6	6
133	Radiation theory comparison for magnetoacoustic tomography with magnetic induction (MAT-MI). Science Bulletin, 2014, 59, 3246-3254.	1.7	6
134	Enhanced ultrasonic focusing and temperature elevation <i>via</i> a therapeutic ultrasonic transducer with sub-wavelength periodic structure. Applied Physics Letters, 2017, 111, .	1.5	6
135	Ambient Pressure Evaluation Through Sub-Harmonic Response ofÂChirp-Sonicated Microbubbles. Ultrasound in Medicine and Biology, 2017, 43, 332-340.	0.7	6
136	Regulation of multiple off-axis acoustic vortices with a centered quasi-plane wave. Journal of Applied Physics, 2018, 124, .	1.1	6
137	<i>In vivo</i> evaluation of two-dimensional temperature variation in perirenal fat of pigs with B-mode ultrasound. Journal of Applied Physics, 2019, 126, .	1.1	6
138	Enantioselective dicarbofunctionalization of (<i>E</i>)-alkenyloxindoles with pyridinium salts by chiral Lewis acid/photo relay catalysis. Chemical Communications, 2020, 56, 12757-12760.	2.2	6
139	Fourier Acoustical Tweezers: Synthesizing Arbitrary Radiation Force Using Nonmonochromatic Waves on Discrete-Frequency Basis. Physical Review Applied, 2021, 15, .	1.5	6
140	Quasi-Bessel Acoustic-Vortex Beams Constructed by the Line-Focused Phase Modulation for a Ring Array of Sectorial Planar Transducers. IEEE Transactions on Ultrasonics, Ferroelectrics, and Frequency Control, 2022, 69, 377-385.	1.7	6
141	Third order harmonic imaging for biological tissues using three phase-coded pulses. Ultrasonics, 2006, 44, e61-e65.	2.1	5
142	Nonlinear oscillation of pathological vocal folds during vocalization. Science China: Physics, Mechanics and Astronomy, 2013, 56, 1324-1328.	2.0	5
143	Finite element modeling of acoustic wave propagation and energy deposition in bone during extracorporeal shock wave treatment. Journal of Applied Physics, 2013, 113, .	1.1	5
144	Real-Time Monitoring and Quantitative Evaluation of Cavitation Bubbles Induced by High Intensity Focused Ultrasound Using B-Mode Imaging. Chinese Physics Letters, 2014, 31, 034302.	1.3	5

#	Article	IF	CITATIONS
145	Nonlinear response of ultrasound contrast agent microbubbles: From fundamentals to applications. Chinese Physics B, 2016, 25, 124308.	0.7	5
146	Multi-relaxation-time lattice Boltzmann modeling of the acoustic field generated by focused transducer. International Journal of Modern Physics C, 2017, 28, 1750038.	0.8	5
147	Accurate acoustic power measurement for low-intensity focused ultrasound using focal axial vibration velocity. Journal of Applied Physics, 2017, 122, 014901.	1.1	5
148	A nonlinear approach to identify pathological change of thyroid nodules based on statistical analysis of ultrasound RF signals. Scientific Reports, 2017, 7, 16930.	1.6	5
149	Low-intensity pulsed ultrasound inhibits adipogenic differentiation via HDAC1 signalling in rat visceral preadipocytes. Adipocyte, 2019, 8, 292-303.	1.3	5
150	Enhancement of the polymerase chain reaction by tungsten disulfide. RSC Advances, 2019, 9, 9373-9378.	1.7	5
151	Manipulating the regioselectivity of a Solanum lycopersicum epoxide hydrolase for the enantioconvergent synthesis of enantiopure alkane- and alkene-1,2-diols. Catalysis Science and Technology, 2020, 10, 5886-5895.	2.1	5
152	Pulling force of acoustic-vortex beams on centered elastic spheres based on the annular transducer model*. Chinese Physics B, 2020, 29, 054302.	0.7	5
153	Lamb wave coupled resonance for SAW acoustofluidics. Applied Physics Letters, 2021, 118, .	1.5	5
154	Theory of acoustophoresis in counterpropagating surface acoustic wave fields for particle separation. Physical Review E, 2021, 103, 033104.	0.8	5
155	p38 MAPK signaling is a key mediator for low-intensity pulsed ultrasound (LIPUS) in cultured human omental adipose-derived mesenchymal stem cells. American Journal of Translational Research (discontinued), 2019, 11, 418-429.	0.0	5
156	Non-Invasive Local Acoustic Therapy Ameliorates Diabetic Heart Fibrosis by Suppressing ACE-Mediated Oxidative Stress and Inflammation in Cardiac Fibroblasts. Cardiovascular Drugs and Therapy, 2022, 36, 413-424.	1.3	5
157	Phase-coded multi-pulse technique for ultrasonic high-order harmonic imaging of biological tissuesin vitro. Physics in Medicine and Biology, 2007, 52, 1879-1892.	1.6	4
158	Quantitative evaluation of contact stiffness between pressed solid surfaces using dual-frequency ultrasound. Journal of Applied Physics, 2010, 108, 034902.	1.1	4
159	A modeling approach to predict acoustic nonlinear field generated by a transmitter with an aluminum lens. Medical Physics, 2011, 38, 5033-5039.	1.6	4
160	Effects of structural differences of graphene and the preparation strategies on the photocatalytic activity of graphene–TiO2 composite film. Journal of Materials Science: Materials in Electronics, 2017, 28, 4965-4973.	1.1	4
161	Impact of cavitation on lesion formation induced by high intensity focused ultrasound. Chinese Physics B, 2017, 26, 054301.	0.7	4
162	Conductivity Anisotropy Influence on Acoustic Sources for Magnetoacoustic Tomography With Magnetic Induction. IEEE Transactions on Biomedical Engineering, 2018, 65, 2512-2518.	2.5	4

#	Article	IF	CITATIONS
163	Non-invasive treatment efficacy evaluation for high-intensity focused ultrasound therapy using magnetically induced magnetoacoustic measurement. Journal of Applied Physics, 2018, 123, 154901.	1.1	4
164	Random phase screen influence of the inhomogeneous tissue layer on the generation of acoustic vortices. Chinese Physics B, 2018, 27, 034301.	0.7	4
165	Evaluation of Cracks in Metallic Material Using a Self-Organized Data-Driven Model of Acoustic Echo-Signal. Applied Sciences (Switzerland), 2019, 9, 95.	1.3	4
166	Improvement in the catalytic performance of a phenylpyruvate reductase from Lactobacillus plantarum by site-directed and saturation mutagenesis based on the computer-aided design. 3 Biotech, 2021, 11, 69.	1.1	4
167	Simulation and verification of an air-gun array wavelet in time-frequency domain based on van der waals gas equation. Applied Geophysics, 2020, 17, 736-746.	0.1	4
168	Investigation on degradation mechanism of polymer blockages in unconsolidated sandstone reservoirs. E-Polymers, 2020, 20, 55-60.	1.3	4
169	Structure-Guided Regulation in the Enantioselectivity of an Epoxide Hydrolase to Produce Enantiomeric Monosubstituted Epoxides and Vicinal Diols via Kinetic Resolution. Organic Letters, 2022, 24, 1757-1761.	2.4	4
170	Investigation on phase-coded third harmonic imaging for normal and pathological tissues in transmission mode in vitro. Science Bulletin, 2006, 51, 1180-1184.	1.7	3
171	Molecular structure dependence of acoustic nonlinearity parameter <i>B/A</i> for silicone oils. Chinese Physics B, 2014, 23, 054302.	0.7	3
172	Nonlinear acoustic-power measurement based on fundamental focal axial vibration velocity for high-intensity focused ultrasound. Journal of Applied Physics, 2018, 124, 214905.	1.1	3
173	Fractal Dimension Differentiation between Benign and Malignant Thyroid Nodules from Ultrasonography. Applied Sciences (Switzerland), 2019, 9, 1494.	1.3	3
174	A note on wind velocity and pressure spectra inside compact spherical porous microphone windscreens. Journal of the Acoustical Society of America, 2020, 147, EL43-EL49.	0.5	3
175	A three-dimensional electrode fabricated by electrophoretic deposition of graphene on nickel foam for structural supercapacitors. New Journal of Chemistry, 2021, 45, 18567-18574.	1.4	3
176	Laboratory Experimental Optimization of Gel Flooding Parameters to Enhance Oil Recovery during Field Applications. ACS Omega, 2021, 6, 14968-14976.	1.6	3
177	Effect of esterification crosslinking on interfacial heat transfer between graphene and phase change material. Composite Interfaces, 2021, 28, 1121-1135.	1.3	3
178	Frequency dependence of the acoustic field generated from a spherical cavity transducer with open ends. AIP Advances, 2015, 5, 127218.	0.6	2
179	Controllable growth of graphene dendrite and application to electrochemical capacitors. Journal of Materials Science: Materials in Electronics, 2015, 26, 4337-4343.	1.1	2
180	Acoustic characterization of high intensity focused ultrasound field generated from a transmitter with large aperture. AIP Conference Proceedings, 2017, , .	0.3	2

#	Article	IF	CITATIONS
181	Classification of benign and malignant breast masses using entropy from nonlinear ultrasound radiofrequency signal. Wuli Xuebao/Acta Physica Sinica, 2021, 70, 084302.	0.2	2
182	Weak-focused acoustic vortex generated by a focused ring array of planar transducers and its application in large-scale rotational object manipulation*. Chinese Physics B, 2021, 30, 044302.	0.7	2
183	Structure-guided improvement in the enantioselectivity of an Aspergillus usamii epoxide hydrolase for the gram-scale kinetic resolution of ortho-trifluoromethyl styrene oxide. Enzyme and Microbial Technology, 2021, 146, 109778.	1.6	2
184	An Analytical Solution for Investigating the Characteristics of Tidal Wave and Surge Propagation Associated with Non-Tropical and Tropical Cyclones in the Humen Estuary, Pearl River. Water (Switzerland), 2021, 13, 2375.	1.2	2
185	Recursive algorithm for solving the axial acoustic radiation force exerted on rigid spheres at the focus of acoustic vortex beams. Journal of Applied Physics, 2021, 130, .	1.1	2
186	Facial Features of an Air Gun Array Wavelet in the Time-Frequency Domain Based on Marine Vertical Cables. Journal of Ocean University of China, 2021, 20, 1371-1382.	0.6	2
187	Directional off-axis acoustic-vortex beams passing through a preassigned point. Journal of Applied Physics, 2021, 130, .	1.1	2
188	Enantioselective Biosynthesis of L-Phenyllactic Acid From Phenylpyruvic Acid In Vitro by L-Lactate Dehydrogenase Coupling With Glucose Dehydrogenase. Frontiers in Bioengineering and Biotechnology, 2022, 10, 846489.	2.0	2
189	Optimization of a random linear ultrasonic therapeutic array based on a genetic algorithm. Ultrasonics, 2022, 124, 106751.	2.1	2
190	A novel approach for description of nonlinear field radiated from a concave source with wide aperture angle. Ultrasonics, 2006, 44, e1435-e1438.	2.1	1
191	Time-frequency analysis of SH waves in an isotropic plate bordered with one elastic solid layer. Science Bulletin, 2006, 51, 2041-2045.	1.7	1
192	The nonlinear oscillation of encapsulated microbubbles in ultrasound contrast agents. AIP Conference Proceedings, 2006, , .	0.3	1
193	Estimation of the tissue lesion induced by a transmitter with aluminium lens. Journal of Physics: Conference Series, 2011, 279, 012020.	0.3	1
194	Investigation on the relationship between overpressure and sub-harmonic response from encapsulated microbubbles. Chinese Physics B, 2014, 23, 104302.	0.7	1
195	Dynamics of Targeted Microbubble Adhesion Under Pulsatile Compared with Steady Flow. Ultrasound in Medicine and Biology, 2014, 40, 2445-2457.	0.7	1
196	Overpressure Dependence of Sub-Harmonic Generation from Contrast Agent SonoVue Microbubbles. Acta Acustica United With Acustica, 2015, 101, 55-61.	0.8	1
197	Overcoming the supercooling of hydrated salts: threeâ€dimensional graphene composite PCMs. Micro and Nano Letters, 2018, 13, 849-852.	0.6	1
198	Research on a Kaâ€Band MEMS Power Sensor Investigated with an MEMS Cantilever Beam. Chinese Journal of Electronics, 2020, 29, 378-384.	0.7	1

#	Article	IF	CITATIONS
199	Low-intensity pulsed ultrasound inhibits IL-1β-induced inflammation of fibroblast-like synoviosytes via NF-κB pathway. Applied Acoustics, 2020, 167, 107384.	1.7	1
200	Nearly perfect kinetic resolution of racemic o-nitrostyrene oxide by AuEH2, a microsomal epoxide hydrolase from Aspergillus usamii, with high enantio- and regio-selectivity. International Journal of Biological Macromolecules, 2021, 169, 1-7.	3.6	1
201	Low-intensity pulsed ultrasound prevents angiotensin II-induced aortic smooth muscle cell phenotypic switch via hampering miR-17-5p and enhancing PPAR-Î ³ . European Journal of Pharmacology, 2021, 911, 174509.	1.7	1
202	Investigation on the effect of active-polymers with different functional groups for EOR. E-Polymers, 2020, 20, 61-68.	1.3	1
203	Separated Respiratory Phases for <i>In Vivo</i> Ultrasonic Thermal Strain Imaging. IEEE Transactions on Ultrasonics, Ferroelectrics, and Frequency Control, 2022, 69, 1219-1229.	1.7	1
204	New insight to experimental study on pore structure of different type reservoirs during alkalineâ€surfactantâ€polymer flooding. Energy Science and Engineering, 2022, 10, 2527-2539.	1.9	1
205	Acoustic Gaussian-Airy beams. Journal Physics D: Applied Physics, 2022, 55, 395109.	1.3	1
206	Measurement of the acoustic nonlinearity parameterB/A of lossy medium in a focused field. Science Bulletin, 2000, 45, 1283-1287.	1.7	0
207	Hysteretic Nonlinearity of Sub-harmonic Emission from Ultrasound Contrast Agent Microbubbles. Chinese Physics Letters, 2011, 28, 044301.	1.3	0
208	Variations of temperature distribution and lesion formation induced by tissue inhomogeneity for therapeutic ultrasound. Proceedings of Meetings on Acoustics, 2013, , .	0.3	0
209	Enhancement effect of ultrasound-induced microbubble cavitation on branched polyethylenimine-mediated Vascular Endothelial Growth Factor 165 (VEGF165)transfection. Proceedings of Meetings on Acoustics, 2013, , .	0.3	0
210	Study of dielectric spectra of ldpe/zeolite nanoscale and micronscale composites. , 2015, , .		0
211	Preparation and properties of BiFeO <inf>3</inf> /LDPE nanocomposite. , 2015, , .		0
212	One-step synthesis of 5-ethyl-2-methylpyridine from NH4HCO3 and C2H5OH under hydrothermal condition. Chemical Research in Chinese Universities, 2015, 31, 249-252.	1.3	0
213	Thermal strain imaging in vivo using interpolated IQ-images. Ultrasonics, 2021, 110, 106292.	2.1	0
214	Quantitative Evaluation of Rotator Cuff Tears Based on Non-linear Statistical Analysis of Ultrasound Radiofrequency Signals. Ultrasound in Medicine and Biology, 2021, 47, 582-589.	0.7	0
215	ACOUSTIC NONLINEAR IMAGING AND ITS APPLICATION IN TISSUE CHARACTERIZATION. , 2007, , 139-153.		0
216	Gram-Scale Synthesis of (R)-P-Chlorophenyl-1,2-Ethanediol at High Concentration by a Pair of Epoxide Hydrolases. Frontiers in Bioengineering and Biotechnology, 2022, 10, 824300.	2.0	0